Electron ionization and the Compton effect in double ionization of helium

James Samson
Department of Physics, University of Nebraska, Lincoln Nebraska

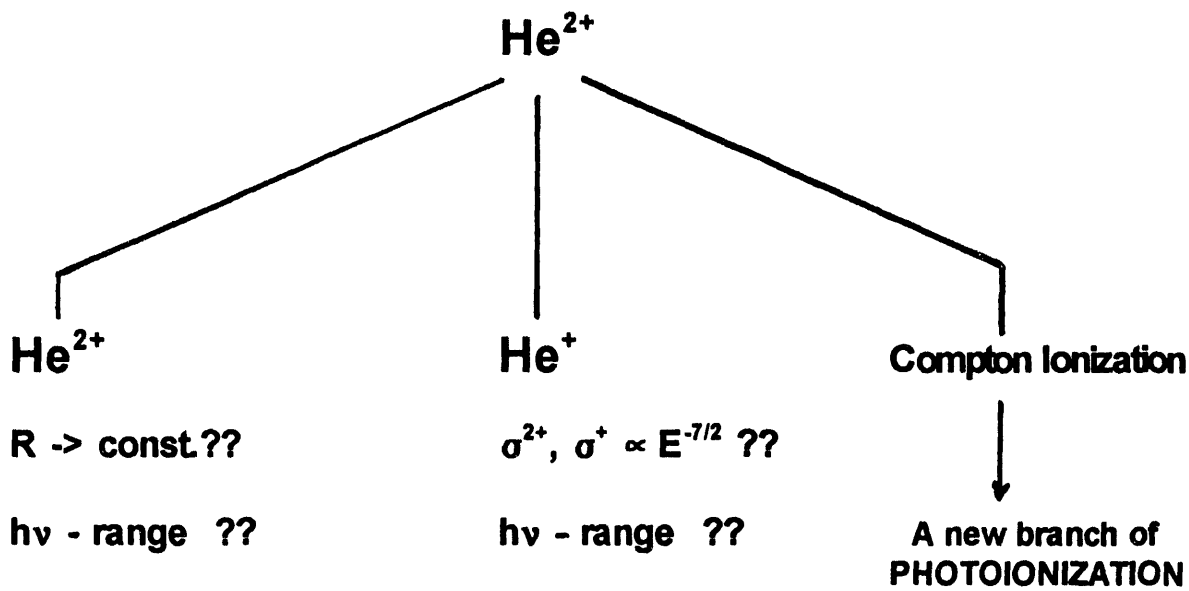

WHAT ARE THE IMPORTANT CORRELATION PROCESSES??

GSC, SO, TS1 (INTERNAL E⁻ COLLISIONS)

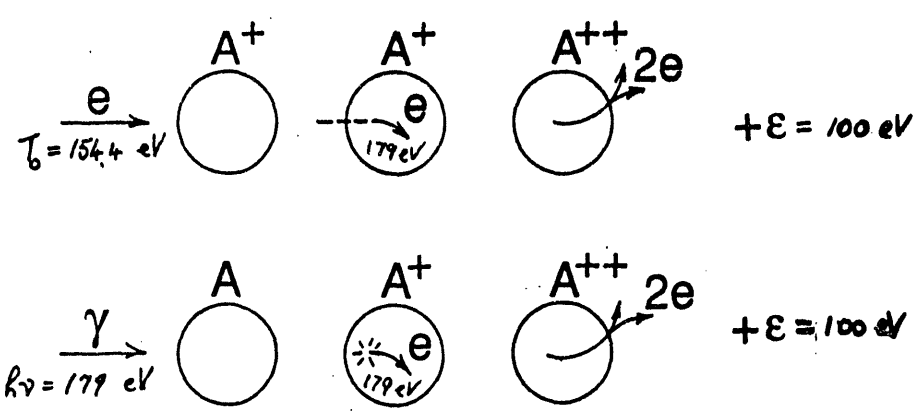

$\sigma_\gamma^{2+} / \sigma_\gamma$ (tot) = σ_e^{+} / const.

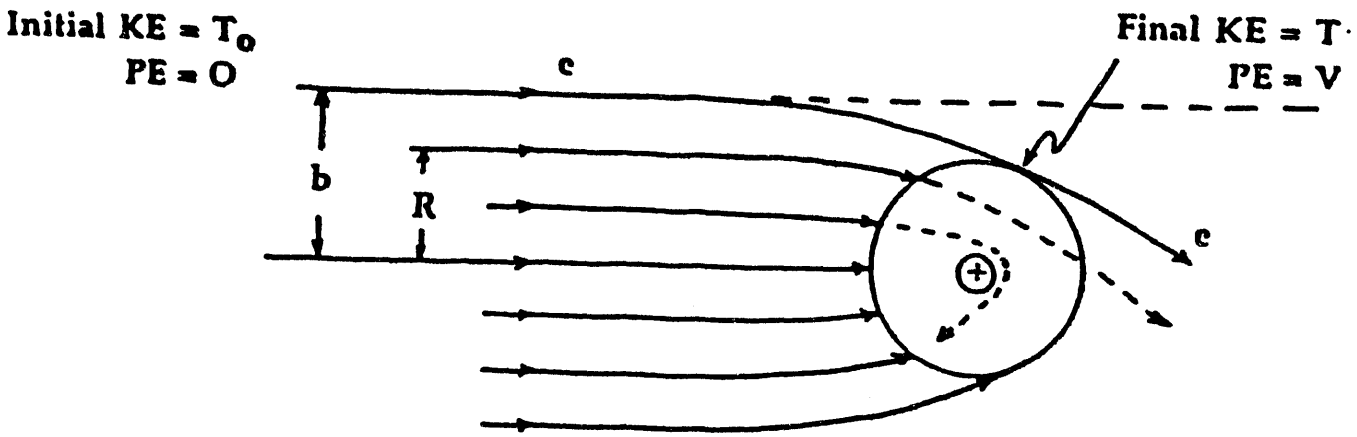

Figure 2. *Schematic diagram for electron impact on an ion showing the impact parameter b for an electron of initial kinetic energy T_0 that can just enter a zone of radius R.*

From the conservation of energy and angular momentum we find that

$$b^2 = R^2\,(1\text{-}V/T_0), \qquad (1)$$

where V is the potential energy of the electron at a distance R from the ionic nucleus. Thus, equating σ_e(abs) to πb^2, Eq.(1) becomes

$$\sigma_\gamma^{2+}/\sigma_\gamma(\text{tot}) = \sigma_e^{+}/k(1\text{-}V/T_0)\,, \qquad (2)$$

where k is a constant that is proportional to πR^2.

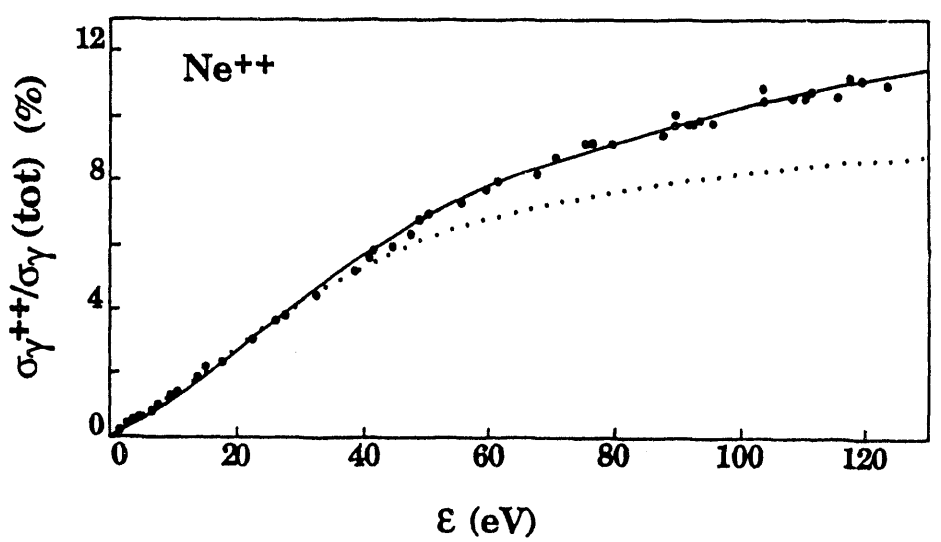

Figure 3. *Neon charge state production ratio*

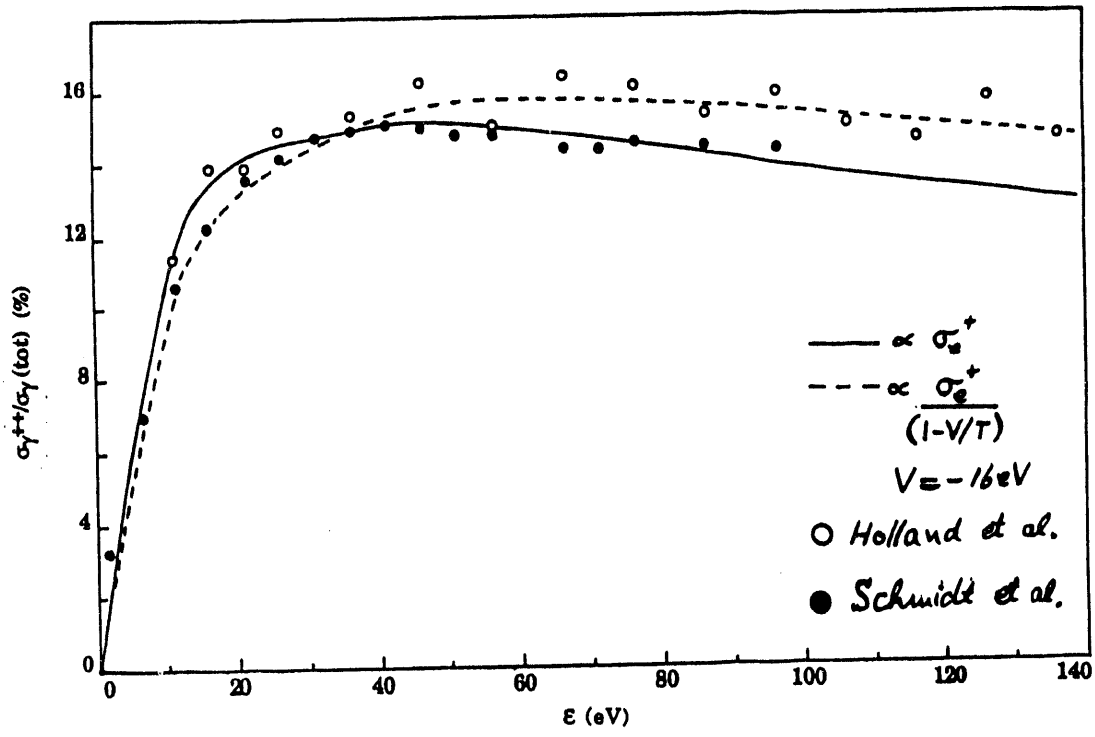

Figure 4. *Helium charge state production ratio at low energies.*

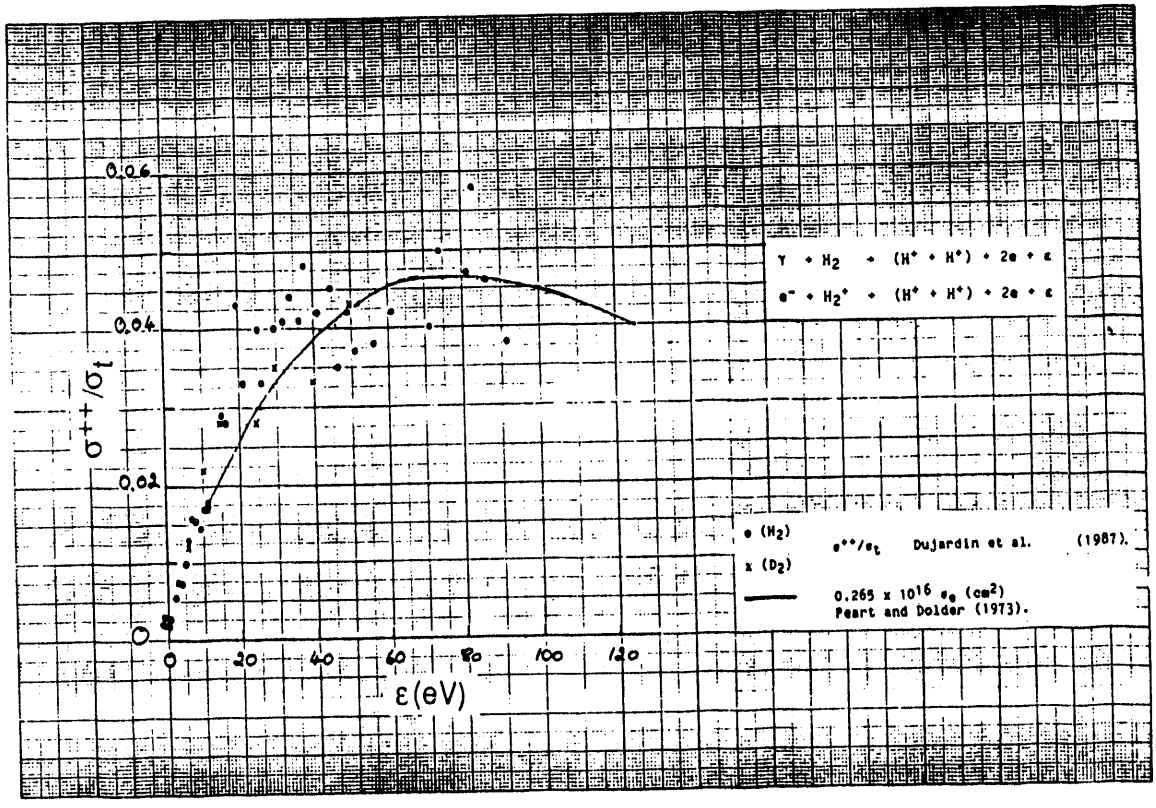

Figure 5. *Helium charge state production ratio; comparison with the theory of Peart & Dolder.*

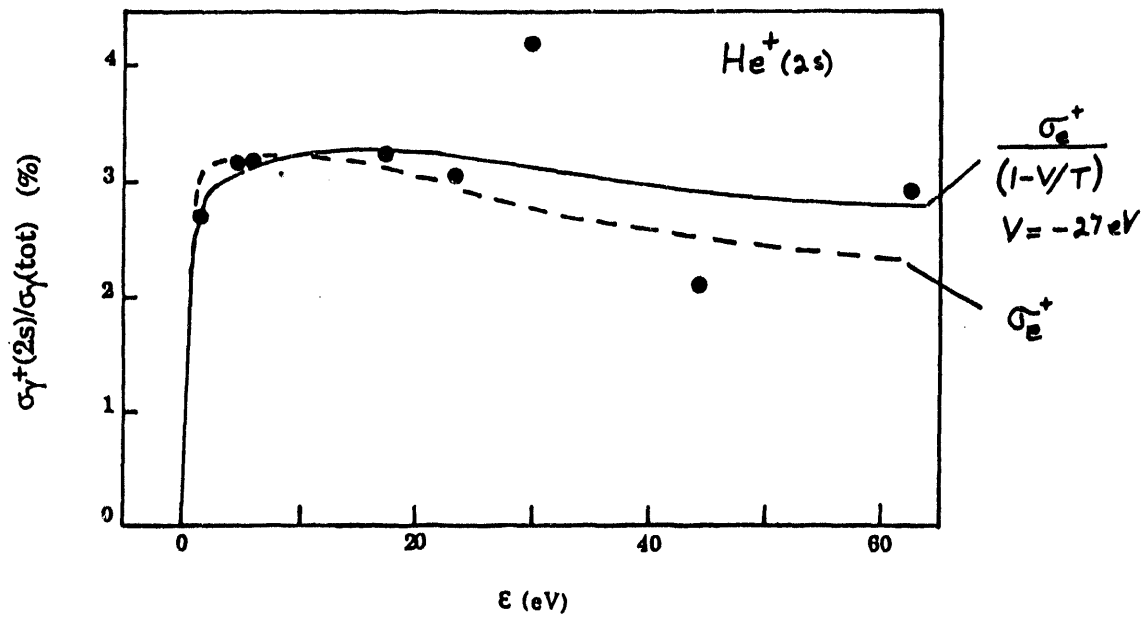

Figure 6. *Helium single ionization compared with electron ionization.*

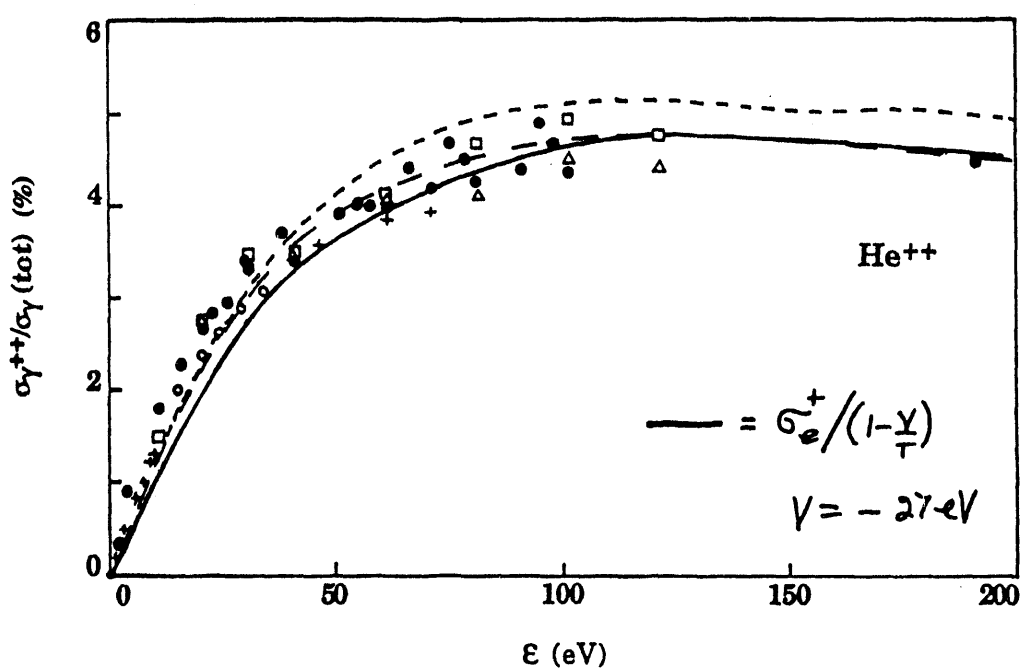

Figure 7. *Helium double ionization compared with electron ionization.*

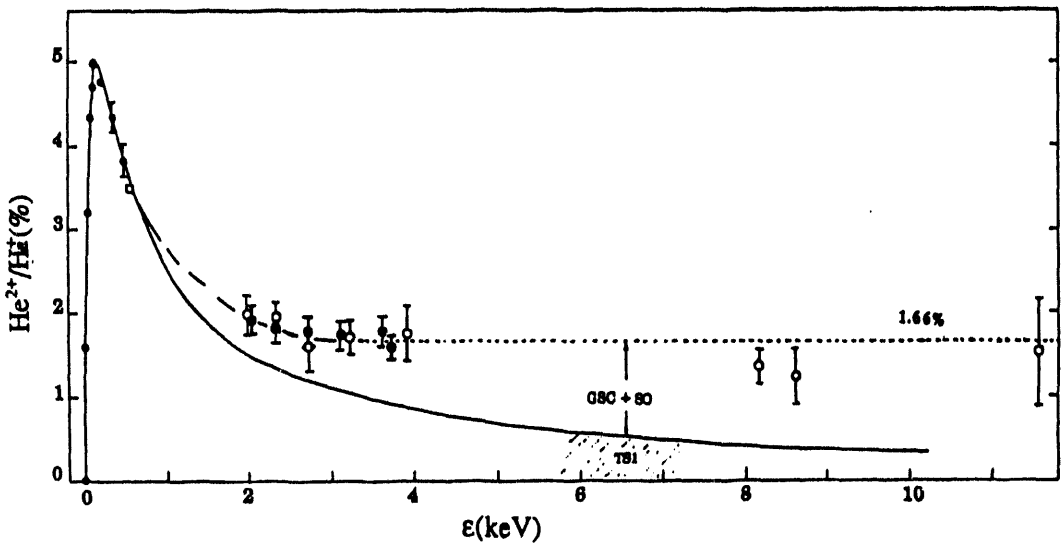

Figure 8. *Measured helium charge state ratio at high energies.*

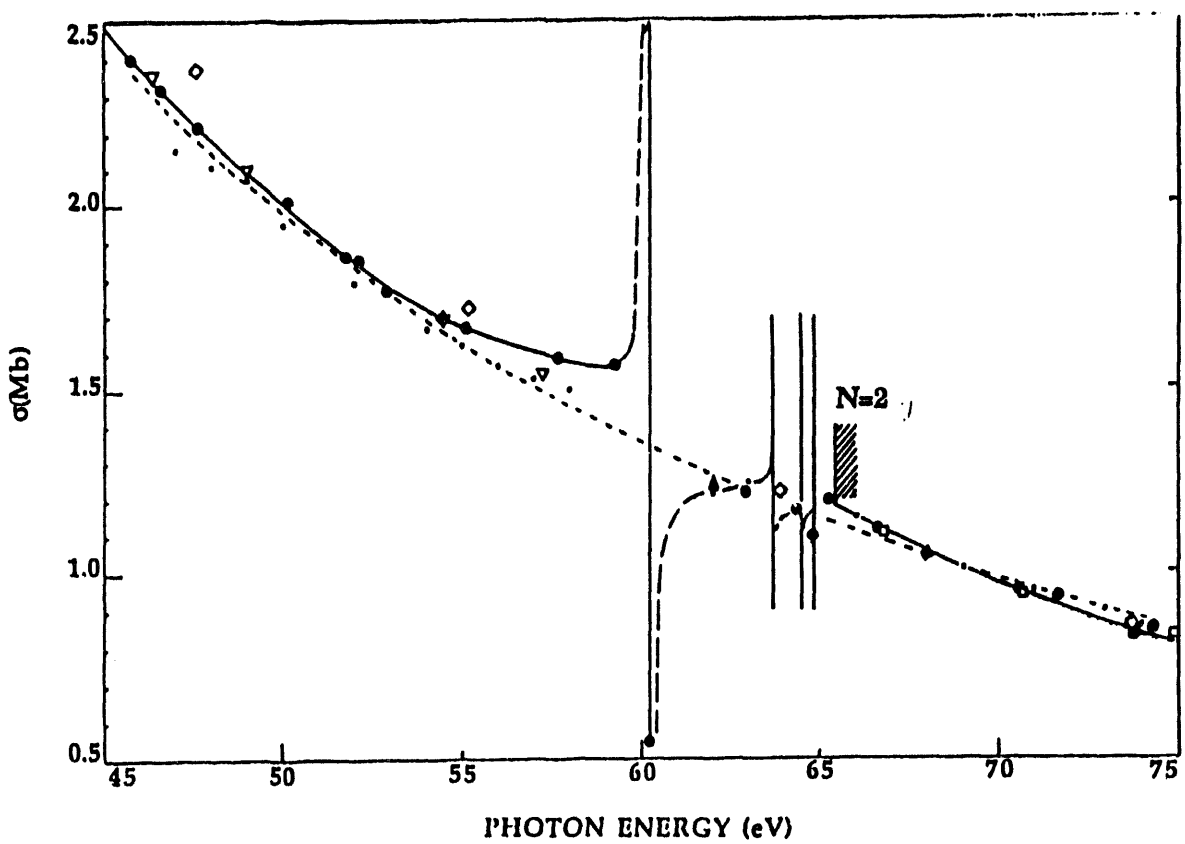

Figure 9. **Photoionization cross sections of He between 45 and 75 eV. Experimental: ●, present data; ——, best fit to data; – – – –, Marr and west (1976); •, Chan et al (1991); △, Morgan and Ederer (1984); □, Watson (1972); Theory: ▽, Altick and Moore (1966); ◆, Wendin (1971); ◇, Amusia et al (1976); — — —, Burke and McVicar (1965) and Fisher and Idrees (1990).**

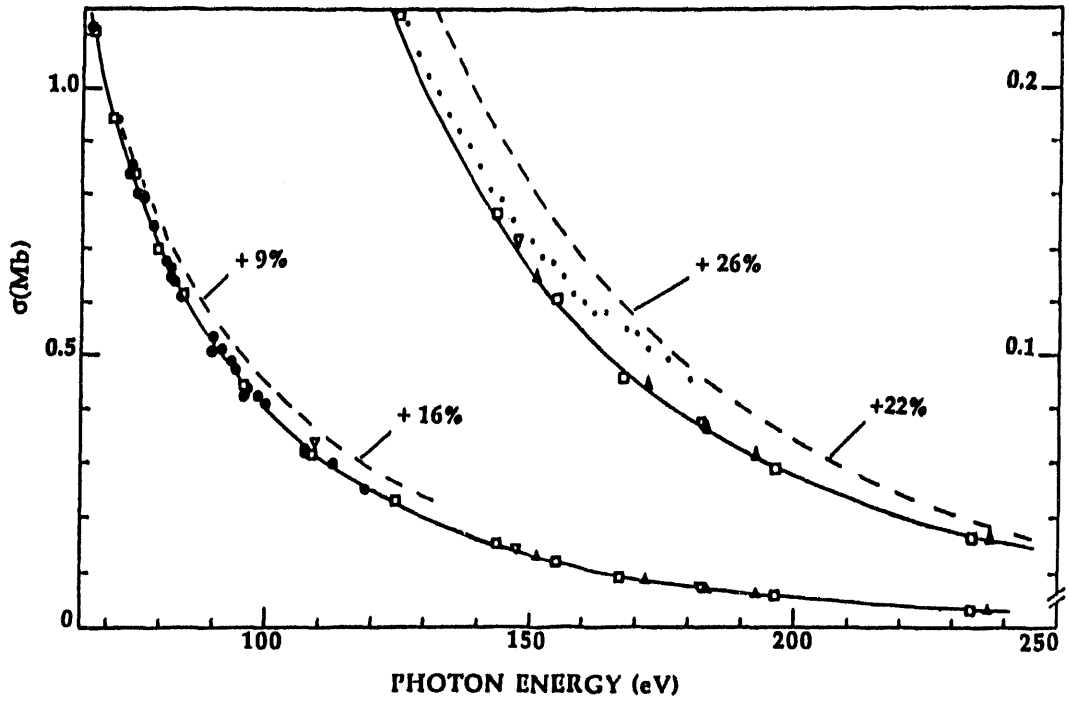

Figure 10.

Photoionization cross sections of He between 70 and 250 eV. ●, present data; —— best fit to data; □, Watson (1972); ▽, Henke (1967); ▲, Denne (1970); – – –, Marr and West (1976); •, Chan et al (1991). The percent values represent the deviation between the present results and the compilation of Marr and West.

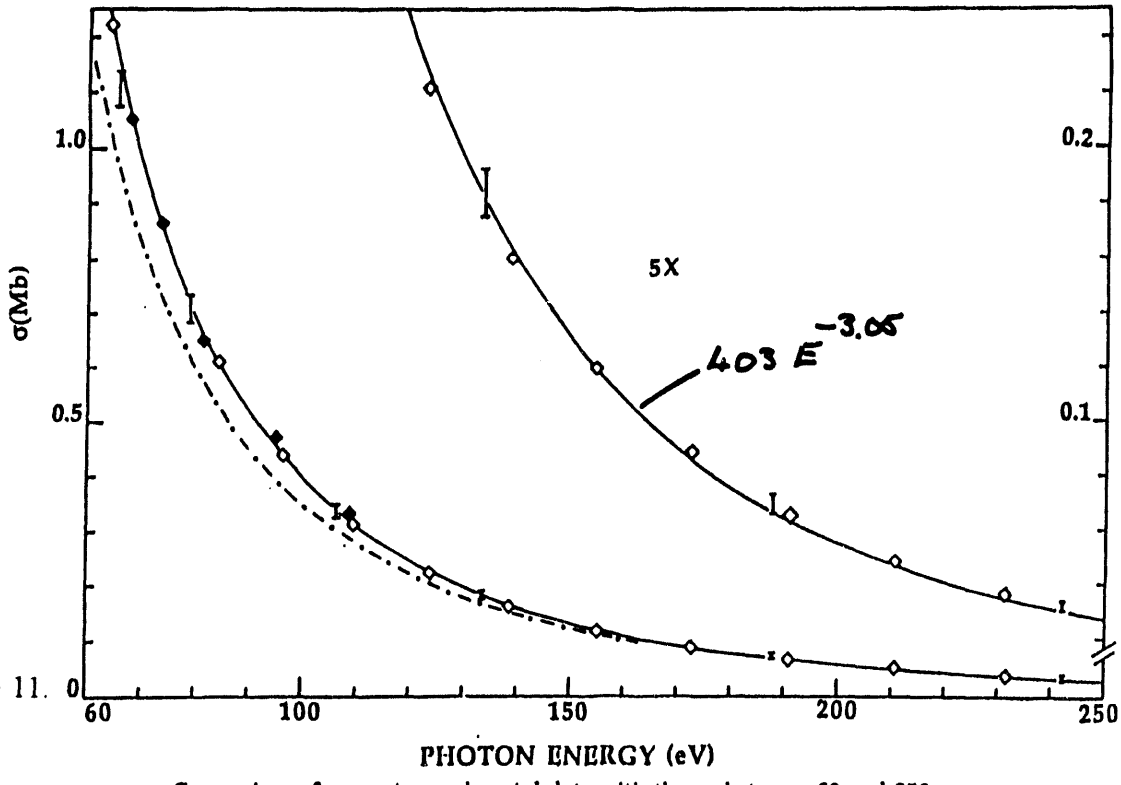

Figure 11.

Comparison of present experimental data with theory between 60 and 250 eV. ——, present results. Theory; ◆, Wendin (1971); ◇, Amusia et al (1976); I, Bell and Kingston (1971); – · – · –, Reilman and Manson (1979).

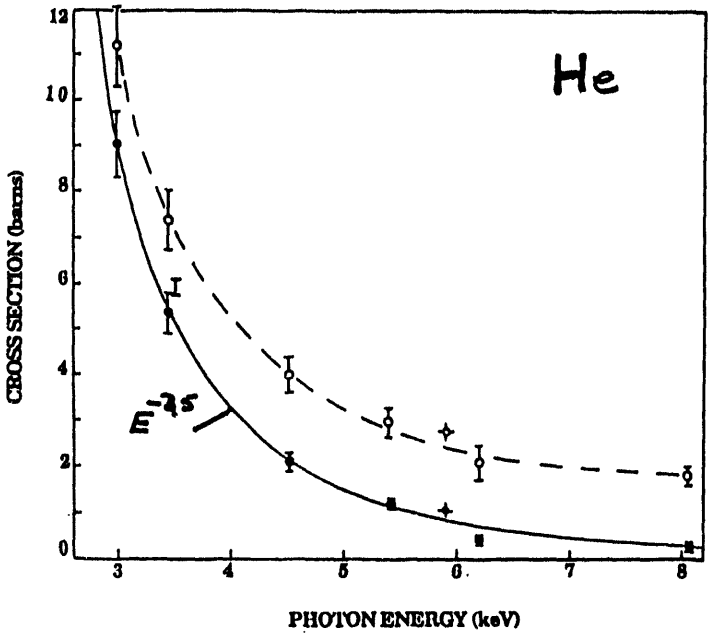

Figure 12.

6. Attenuation and Photoionization data derived from the experimental results of Bearden (1966) and McCrary et al (1970). O and ●, Bearden; ⊹ and ✦, McCrary et al. The dashed line helps to view the attenuation data. The solid line is a best fit to the photoionization data and can be represented by the equation σ(barns) = 410 E(keV)$^{-3.5}$. Theory: Σ, calculated data in the length (upper cap) and velocity (lower cap) approximation at 3.5 keV, Bell and Kingston (1971).

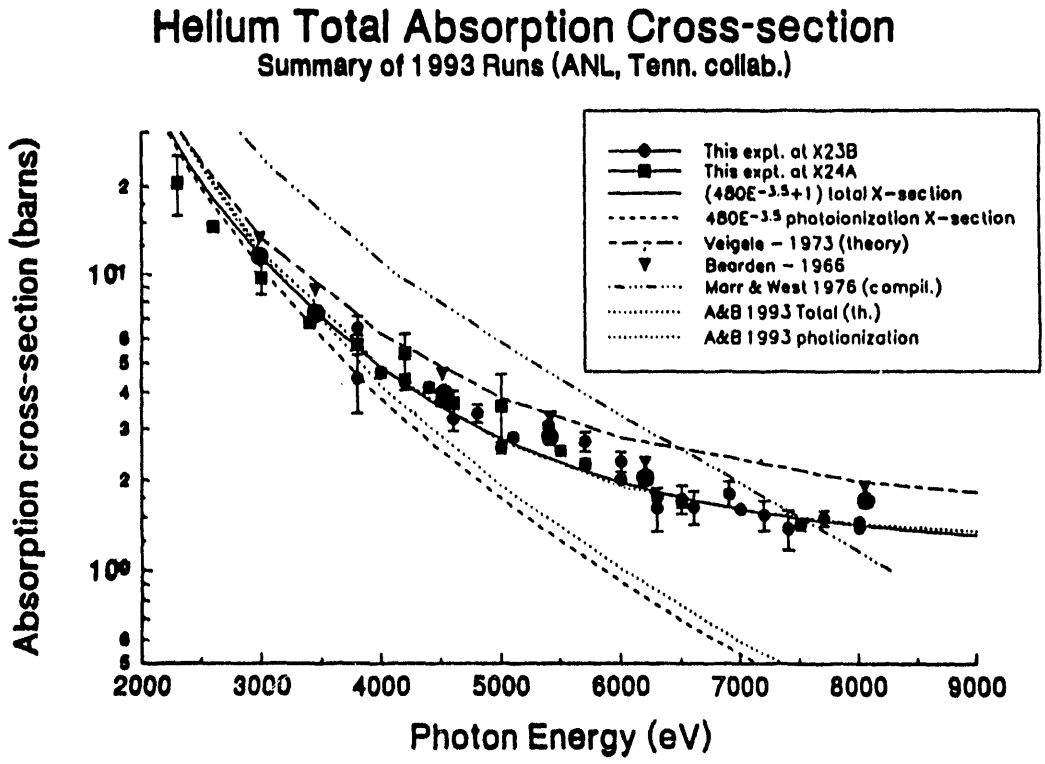

Figure 13. *Measured total absorption cross-section; Azuma et al, preliminary data.*

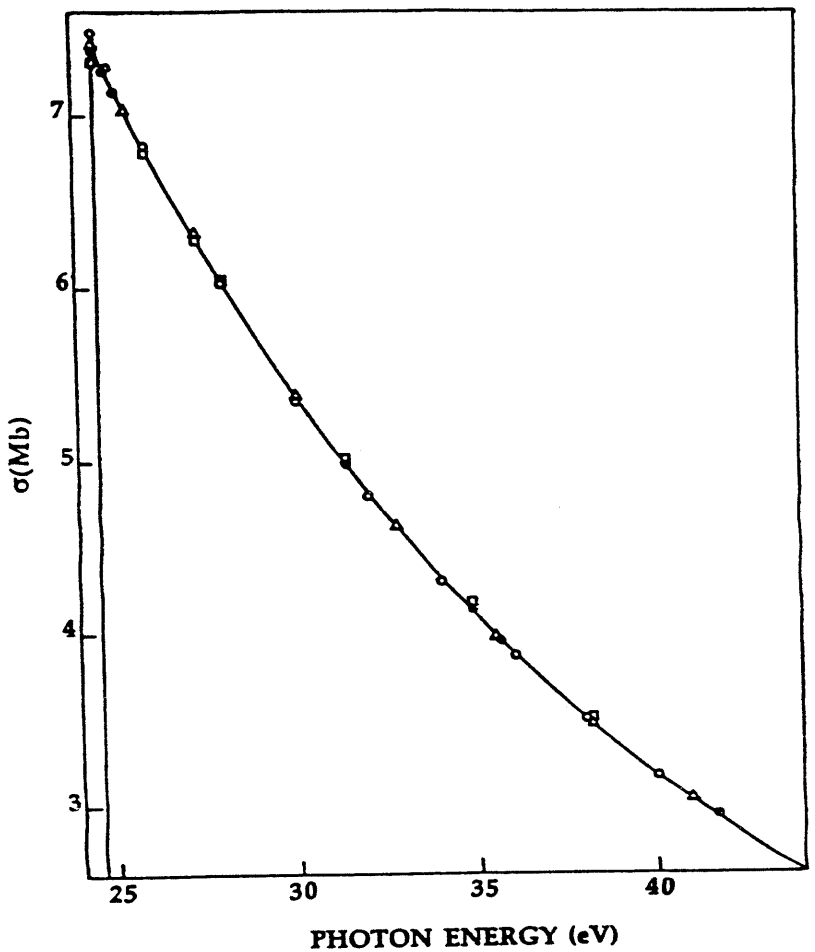

Comparison of present experimental data with theory between 24.6 eV and 44 eV. —— present results. Theory; □, Bell and Kingston (1971); ●, Stewart (1978); ○, Fernley (1987); Δ, Tang et al (1992).

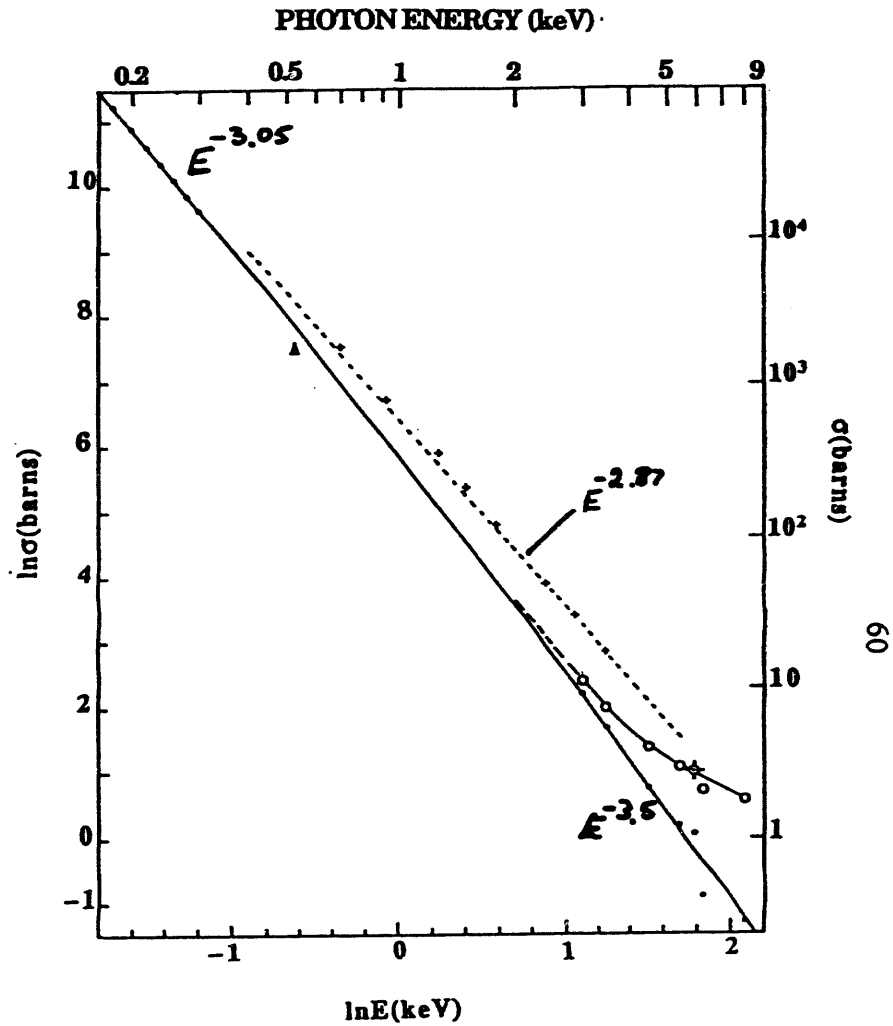

Predicted photoionization cross sections (solid line) between 200 eV and 8 keV. Small dots at low energy, present data; small dots at high energy, derived from Bearden (1966) and McCrary et al (1970); ▲, Denne (1970); Attenuation data: – – – Marr and West (1976); +, Allen (1935); ⊹ McCrary et al; O, derived from Bearden (1966).